Electronic Supporting Information

Forays into Rhodium Macrocyclic Chemistry Stabilized by a P_2N_2 Donor Set. Activation of Dihydrogen and Benzene

*Alyssa Yeo, Corey A. Sanz, and Michael D. Fryzuk**

Department of Chemistry, The University of British Columbia, 2036 Main Mall, Vancouver, BC, V6T 1Z1 CANADA.

Selected NMR Spectra

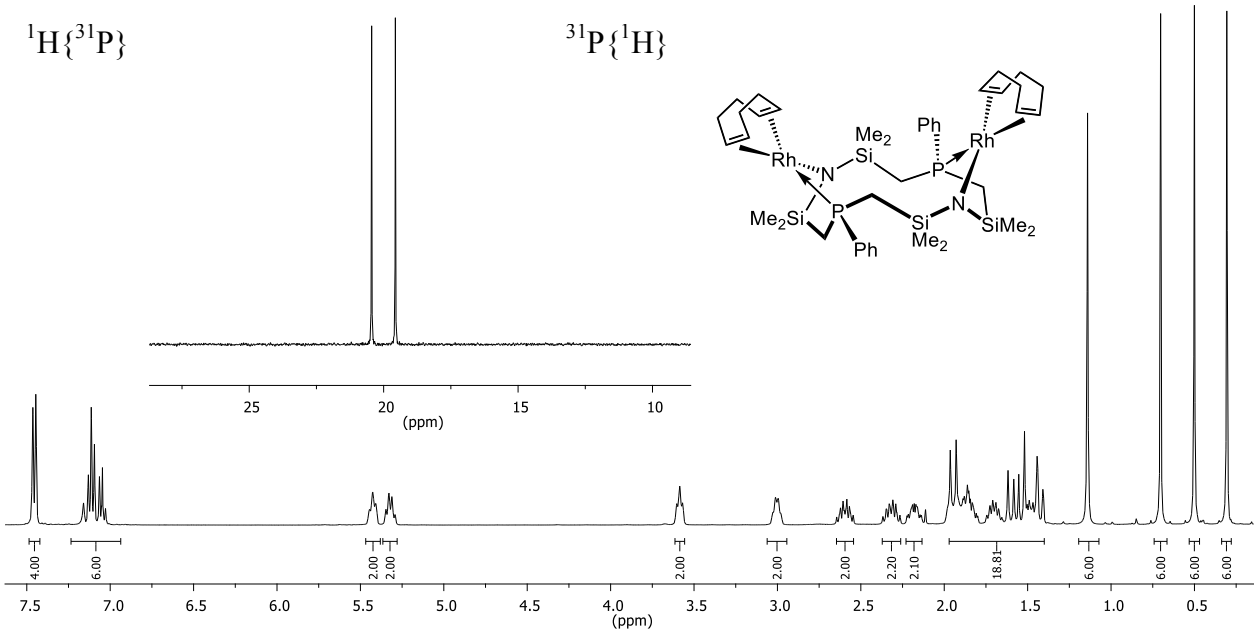

Figure S1 $^{31}P\{^{1}H\}$ NMR (161.9 Hz) spectrum (inset) and $^{1}H\{^{31}P\}$ NMR (400 MHz) spectrum of $[P_2N_2][Rh(COD)]_2$ (**1**) (in C_6D_6).

^{31}P NMR (161.9 MHz, C_6D_6) δ 33.65 (d, J = 95.9 Hz), 21.03 (d, J = 104.8 Hz), 20.60 (d, J = 114.3 Hz).

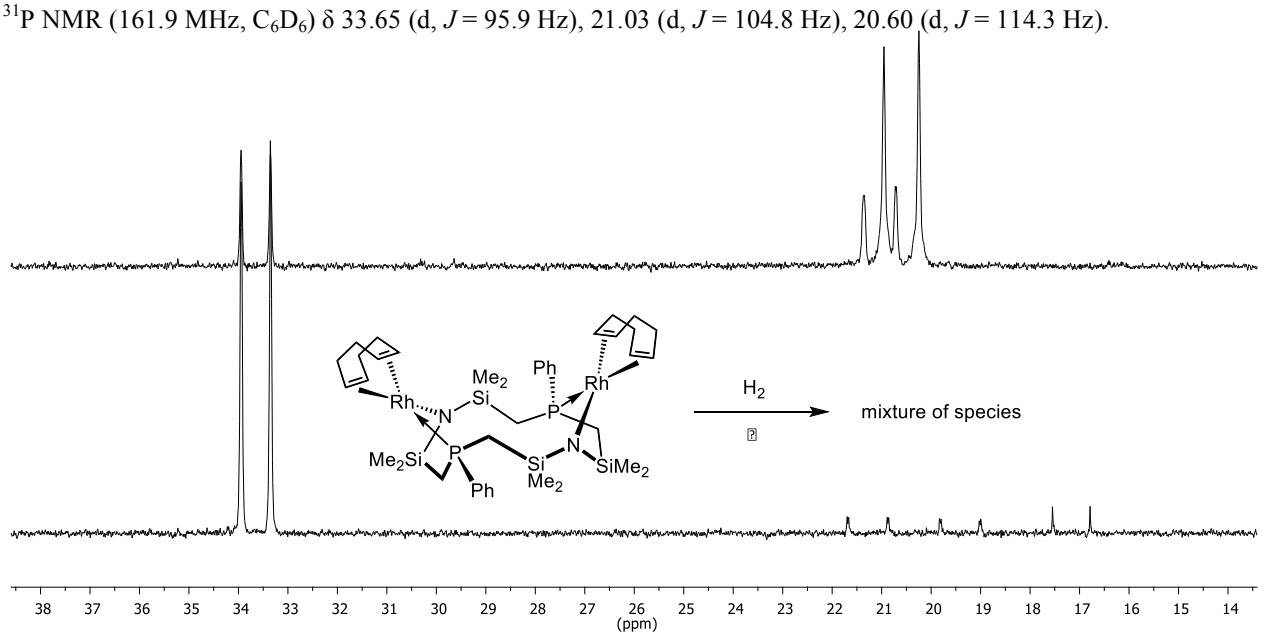

Figure S2 Comparison of the $^{31}P\{^{1}H\}$ NMR spectra (161.9 MHz, C_6D_6) of the material isolated after the treatment of $[P_2N_2][Rh(COD)]_2$ (**1**) with H_2 gas, before heating (top) and after heating at 80 °C for 12 h (bottom).

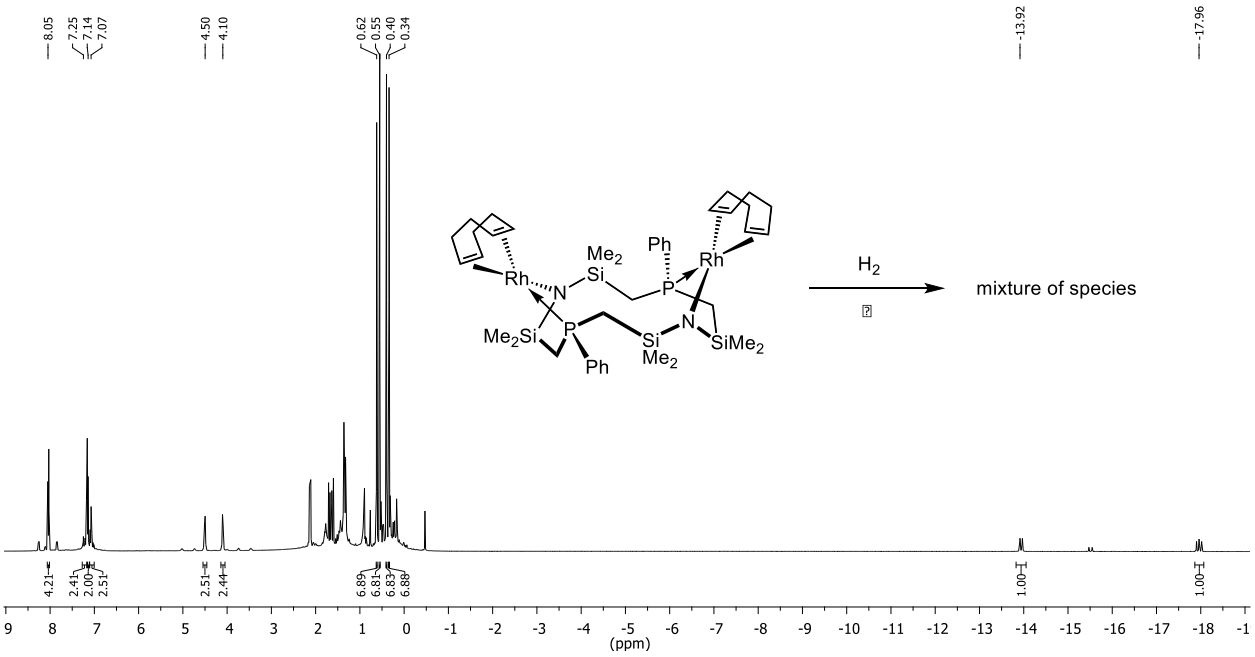

Figure S3 $^{1}H\{^{31}P\}$ NMR spectrum (400 MHz, C_6D_6) of the material isolated after the treatment of $[P_2N_2][Rh(COD)]_2$ (**1**) with H_2 gas, after heating at 80 °C for 12 h.

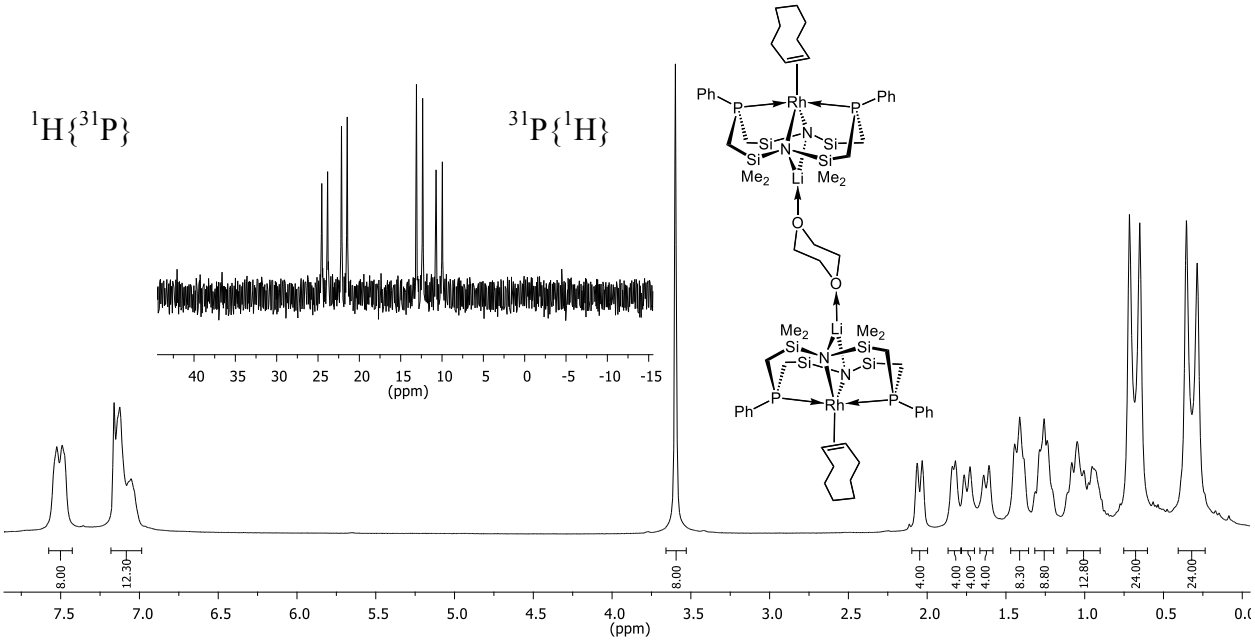

Figure S4 $^{31}P\{^{1}H\}$ NMR (161.9 MHz) spectrum (inset) and $^{1}H\{^{31}P\}$ NMR (400 MHz) spectrum of $([Rh(COE)][P_2N_2]Li)_2$(dioxane) (**2**) (in C_6D_6).

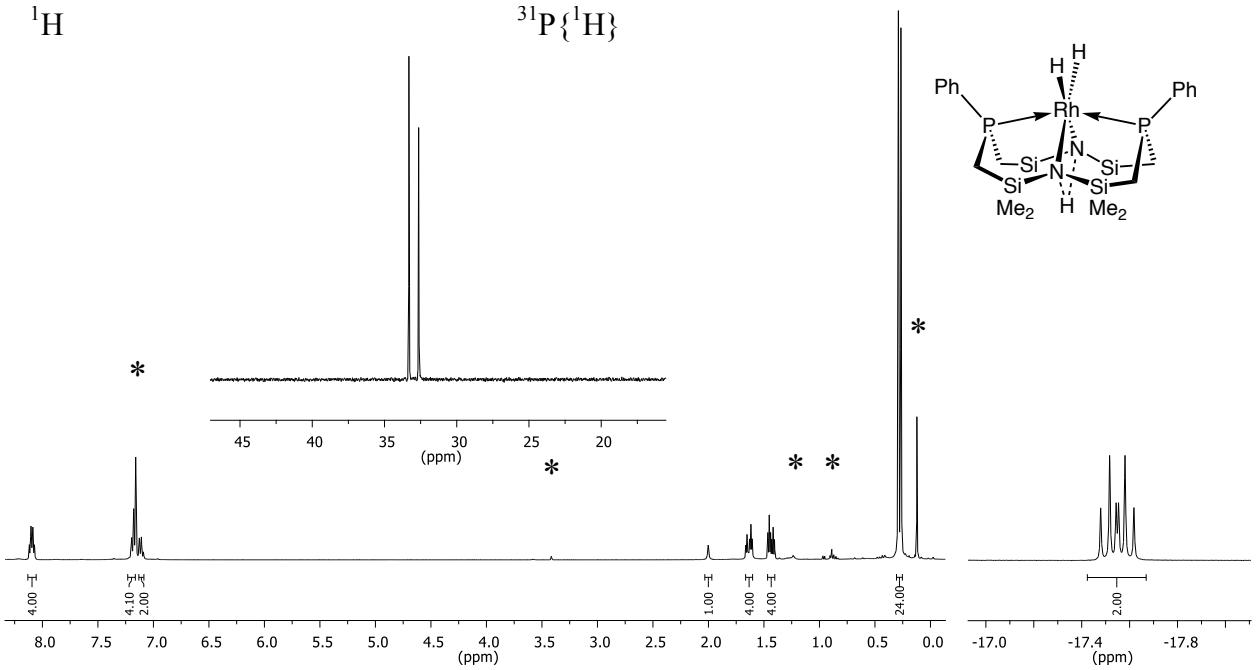

Figure S5 ^{31}P{^{1}H} NMR (161.9 MHz) spectrum (inset) and ^{1}H NMR (400 MHz) spectrum of Rh[P_2N_2H]$(H)_2$ (**3**) (in C_6D_6). (Resonances denoted with (*) indicate residual solvent impurities of hexanes and HMDSO).

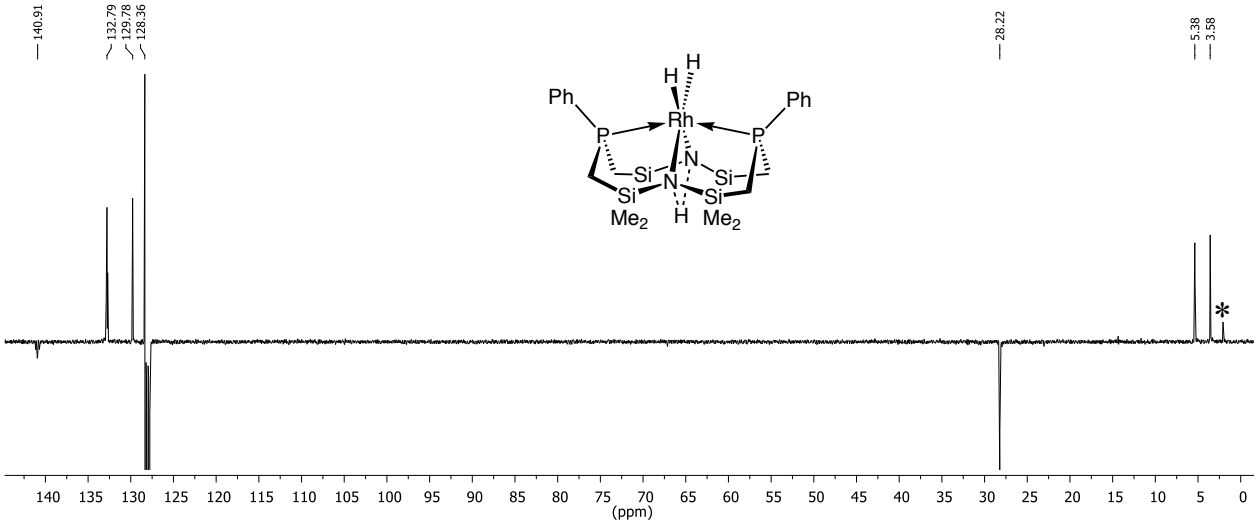

Figure S6 ^{13}C APT NMR spectrum (100.6 MHz, C_6D_6) of Rh[P_2N_2H]$(H)_2$ (**3**) (with methine and methyl carbons in a positive phase and negatively phased quaternary carbons and methylene carbons). (Resonance denoted with (*) corresponds to residual HMDSO).

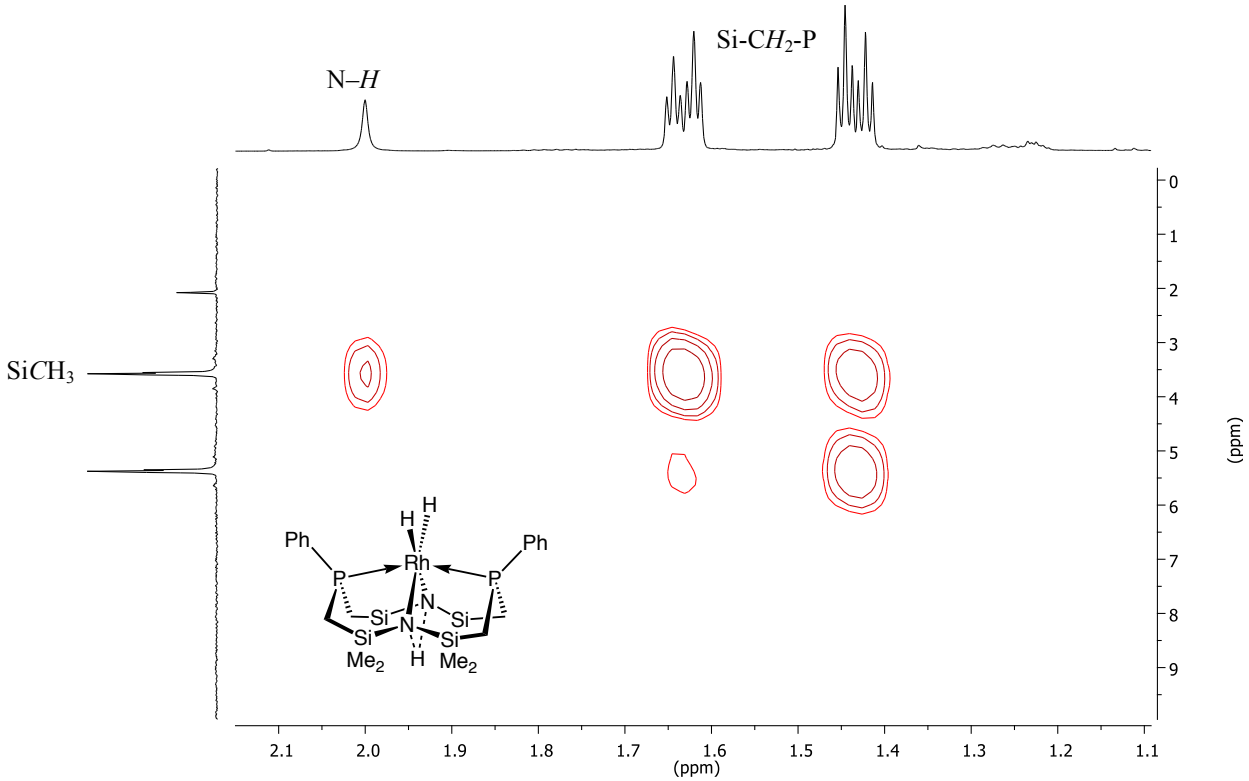

Figure S7 ^{1}H–^{13}C HMBC NMR spectrum (400 MHz ^{1}H and 100.6 MHz ^{13}C external projections, C_6D_6) of $Rh[P_2N_2H](H)_2$ (**3**) displaying a multiple-bond correlation between the N–H proton and silyl methyl carbons.

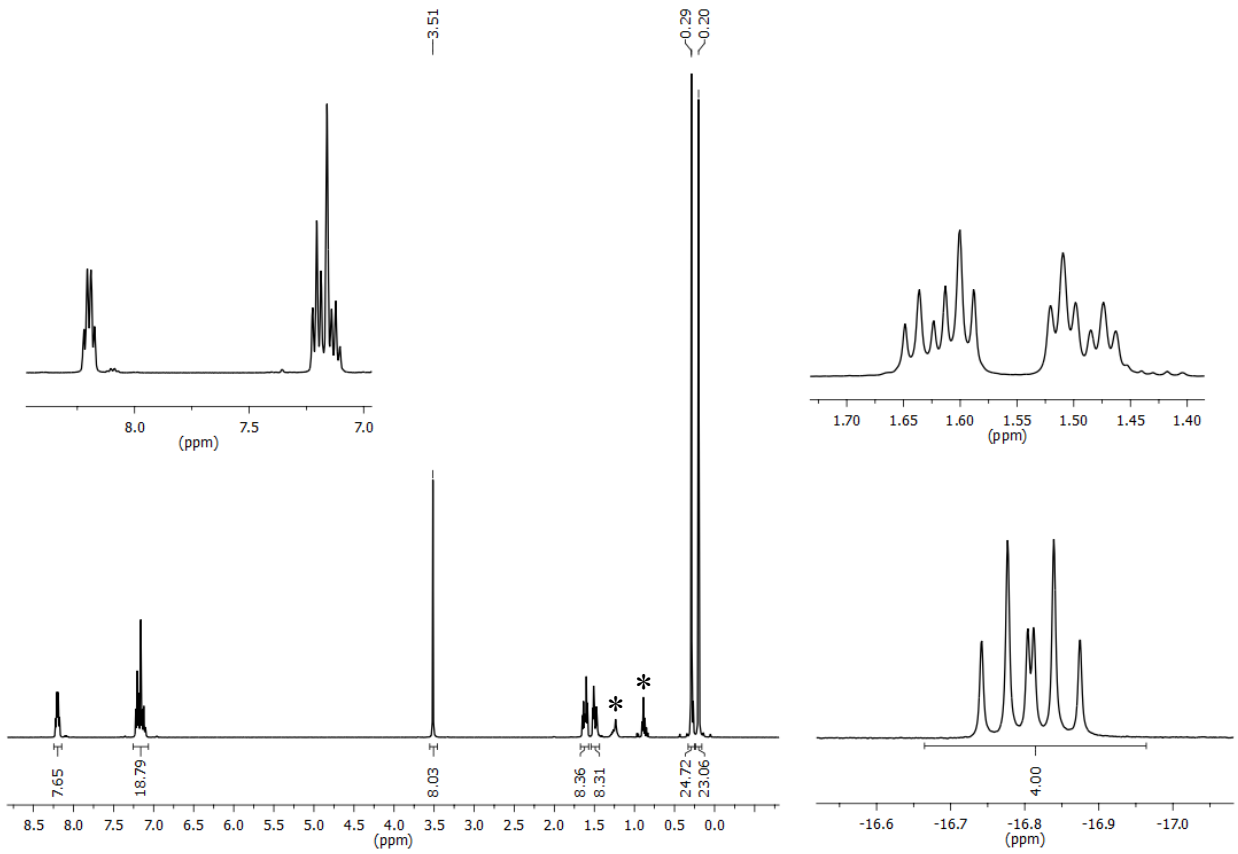

Figure S8 ^{1}H NMR (400 MHz) spectrum of ($[Rh(H)_2][P_2N_2]Li)_2$(dioxane) (**4**) (in C_6D_6). (Resonances denoted with (*) correspond to residual hexanes).

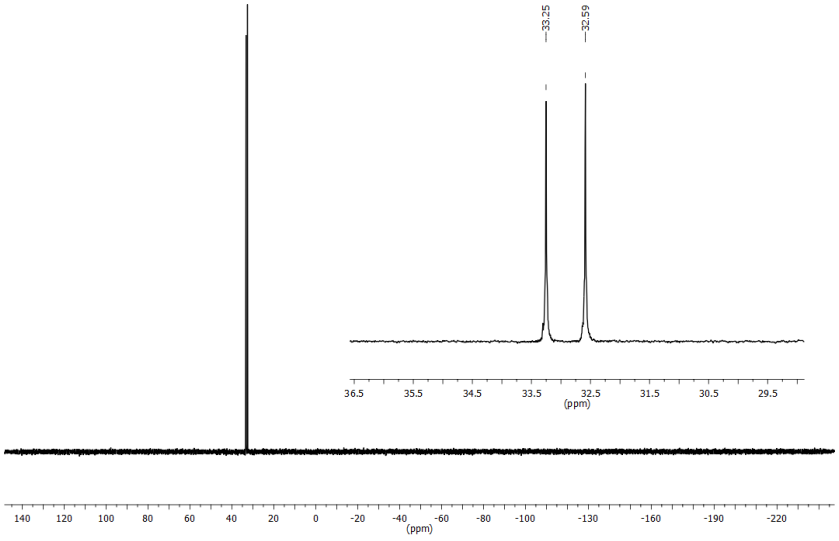

Figure S9 $^{31}P\{^{1}H\}$ NMR (161.9 MHz) spectrum of ($[Rh(H)_2][P_2N_2]Li)_2$(dioxane) (**4**) (in C_6D_6).

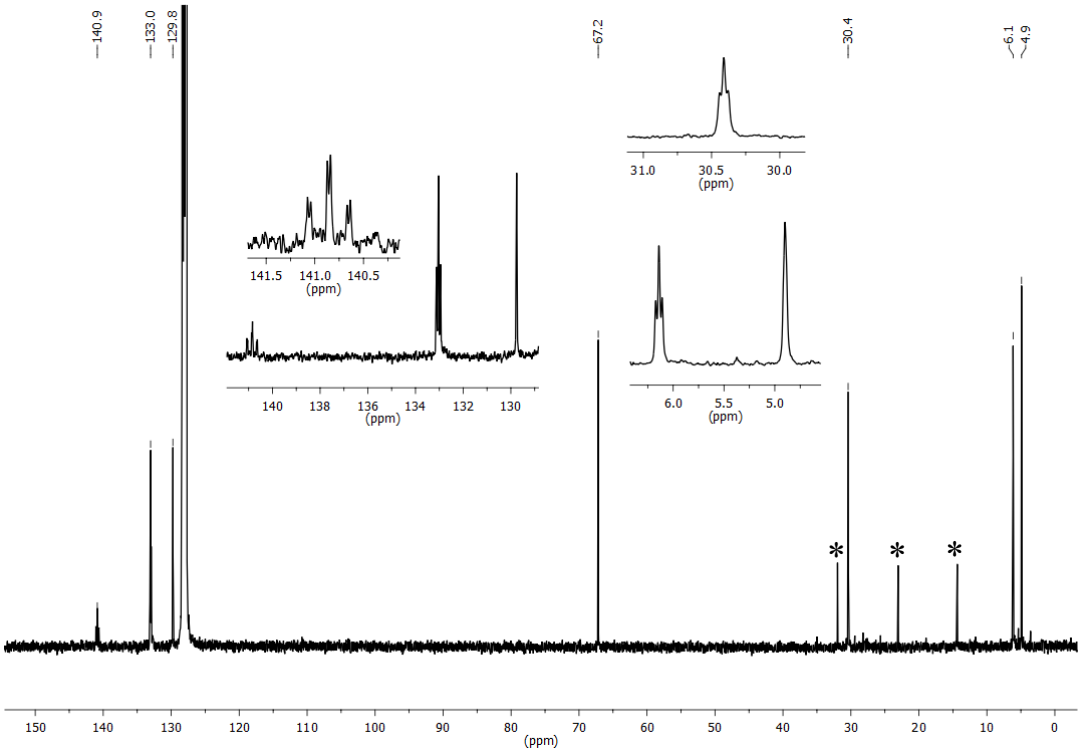

Figure S10 $^{13}C\{^{1}H\}$ NMR (100.6 MHz) spectrum of $([Rh(H)_2][P_2N_2]Li)_2$(dioxane) (**4**) (in C_6D_6). (Resonances denoted with (*) correspond to residual hexanes).

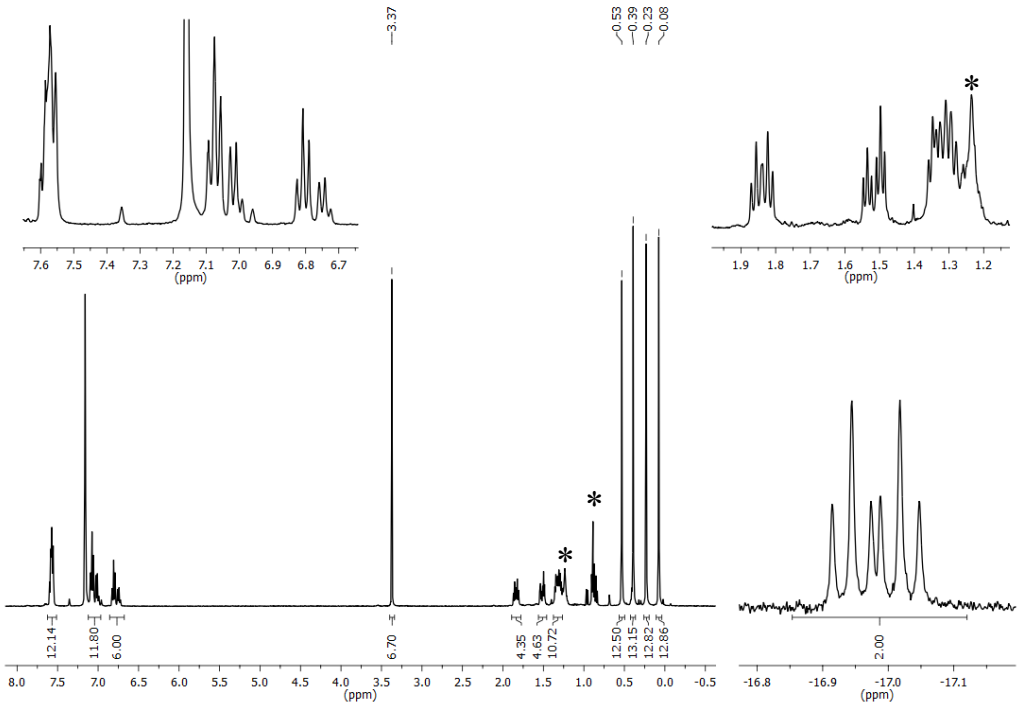

Figure S11 ^{1}H NMR (400 MHz) spectrum of $([Rh(C_6H_5)H][P_2N_2]Li)_2$(dioxane) (**5**) (in C_6D_6). (Resonances denoted with (*) correspond to residual hexanes).

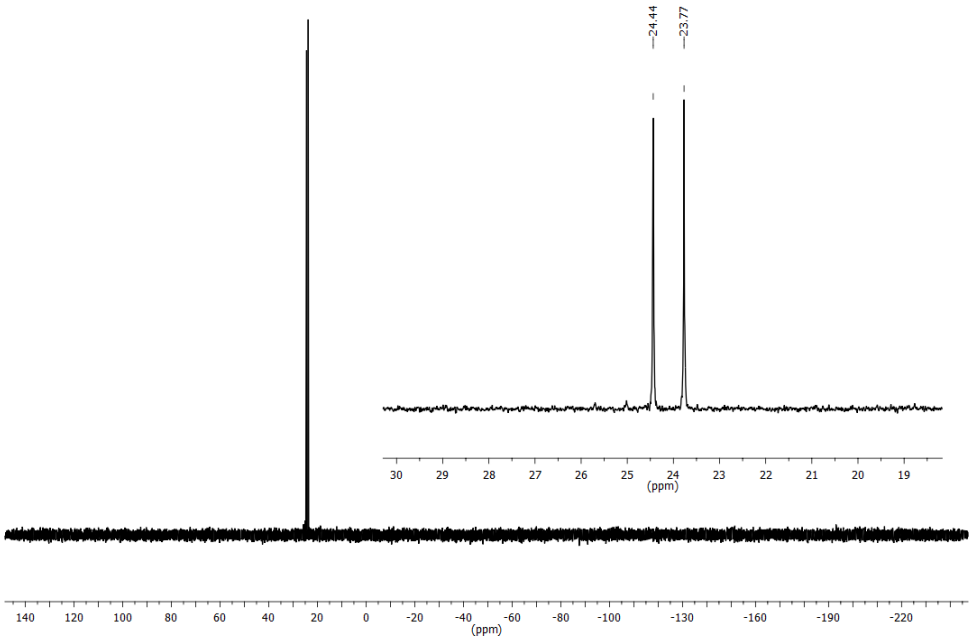

Figure S12 $^{31}P\{^{1}H\}$ NMR (161.9 MHz) spectrum of **[**($[Rh(C_6H_5)H][P_2N_2]Li)_2$(dioxane) (**5**) (in C_6D_6).

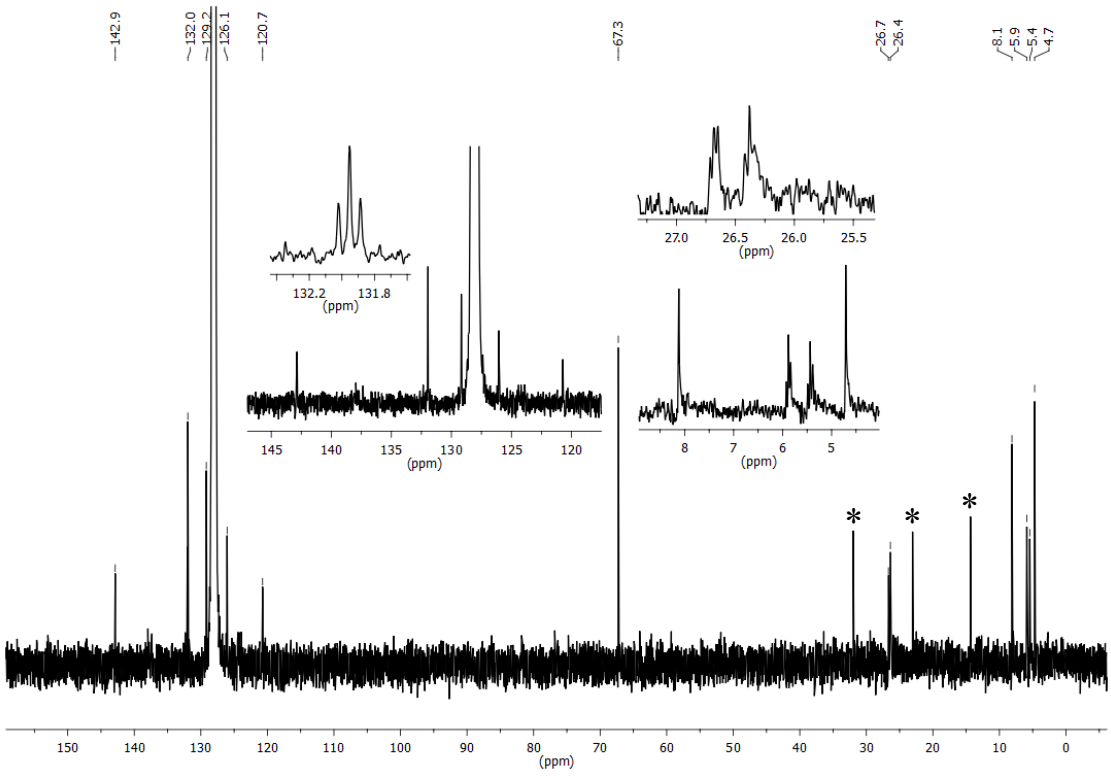

Figure S13 $^{13}C\{^{1}H\}$ NMR (100.6 MHz) spectrum of ($[Rh(C_6H_5)H][P_2N_2]Li)_2$(dioxane) (**5**) (in C_6D_6). (Resonances denoted with (*) correspond to residual hexanes).

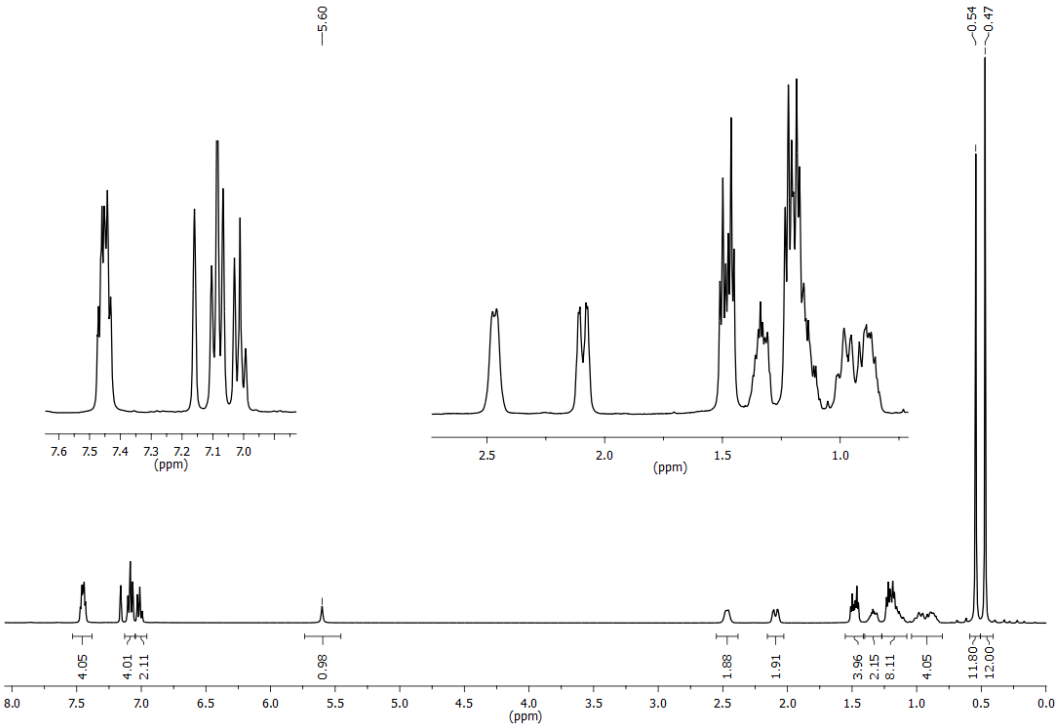

Figure S14 ^{1}H NMR (400 MHz) spectrum of Rh[P_2N_2H](COE) (**6**) (in C_6D_6).

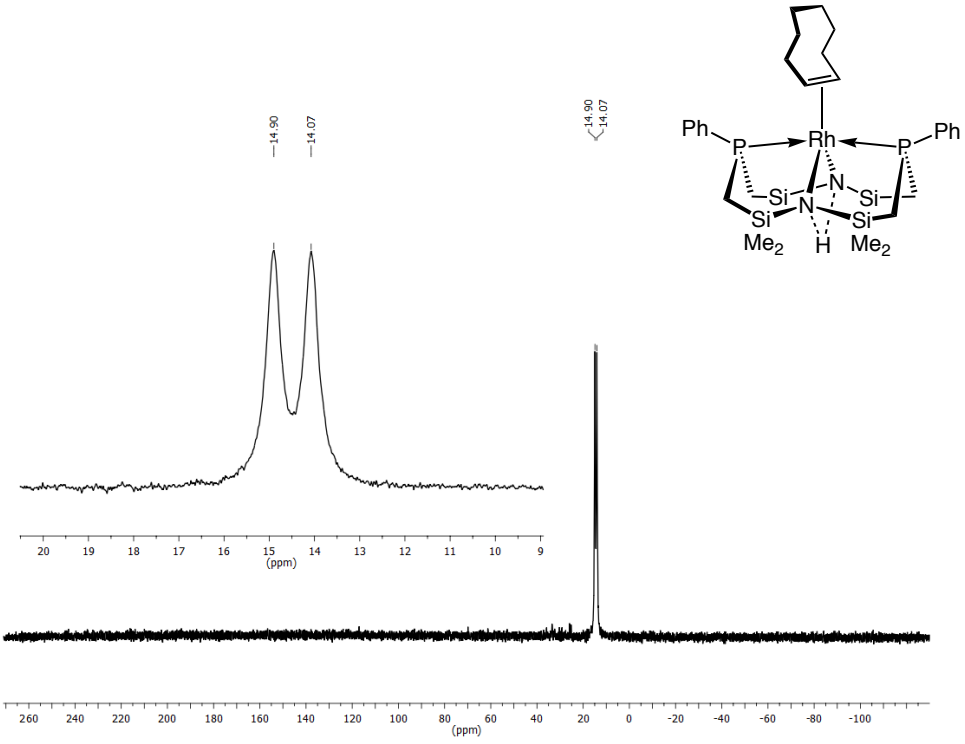

Figure S15 ^{31}P{^{1}H} NMR (161.9 MHz) spectrum of Rh[P_2N_2H](COE) (**6**) (in C_6D_6) at 298K.

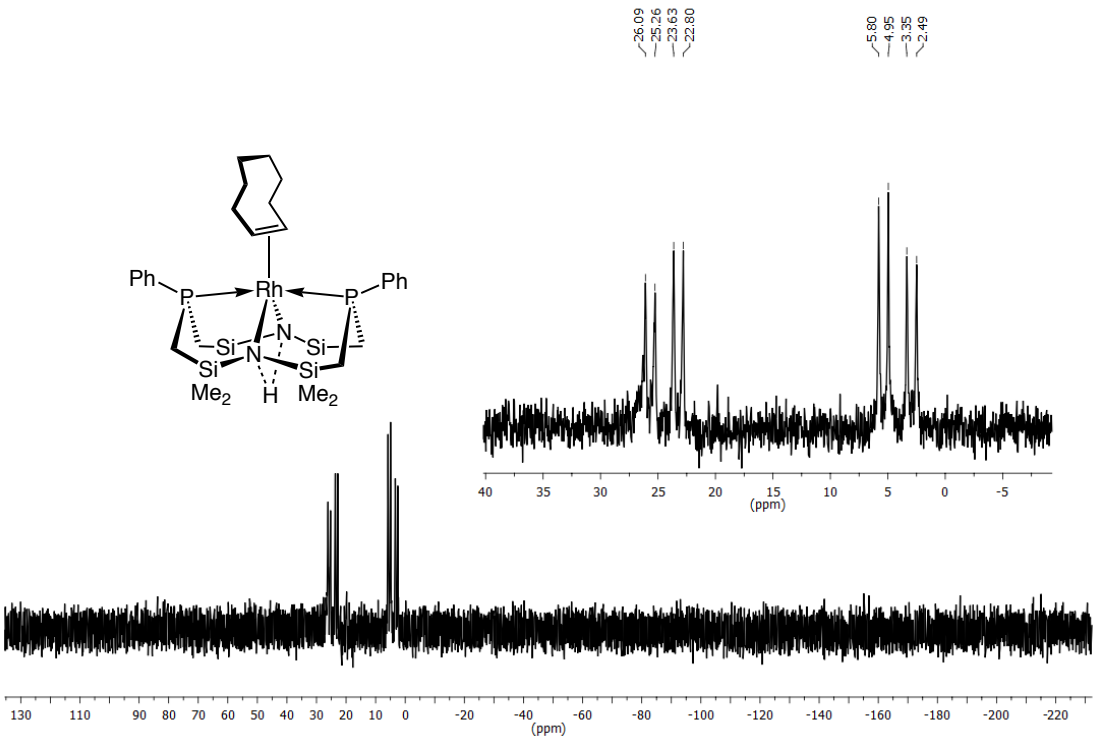

Figure S16 $^{31}P\{^{1}H\}$ NMR (161.9 MHz) spectrum of Rh[P_2N_2H](COE) (**6**) (in toluene-d_8) at 188K.

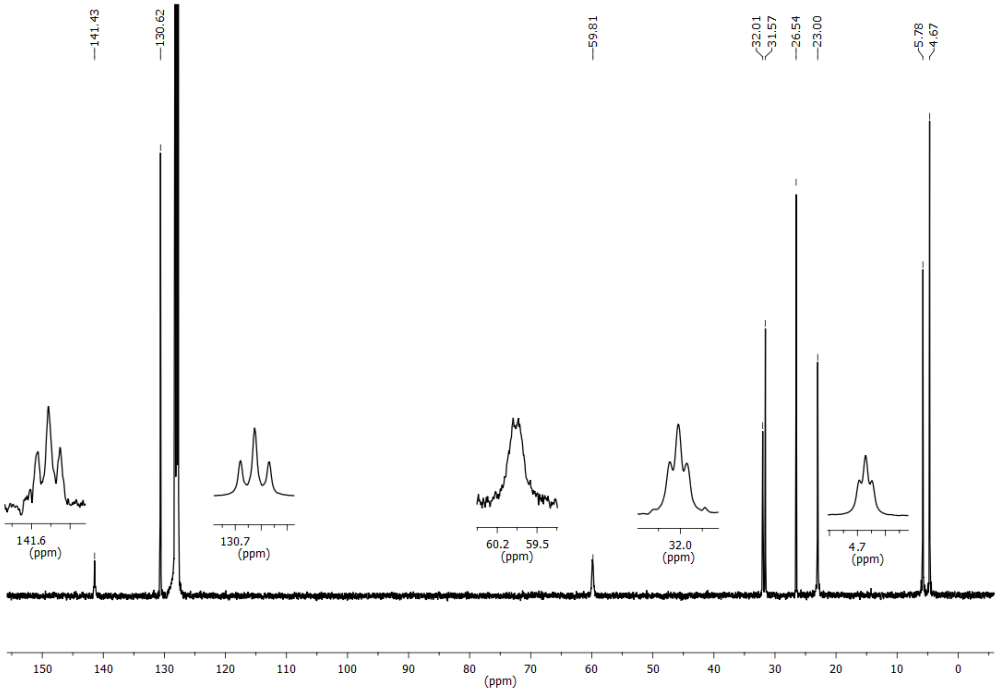

Figure S17 $^{13}C\{^{1}H\}$ NMR (100.6 MHz) spectrum of Rh[P_2N_2H](COE) (**6**) (in C_6D_6).

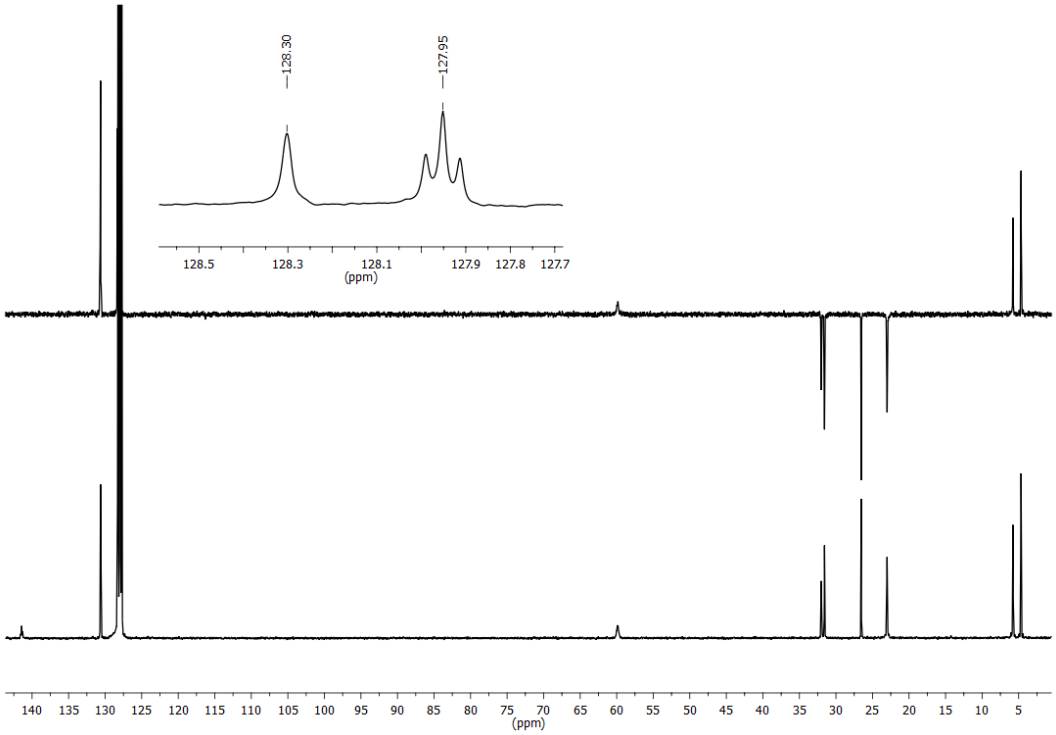

Figure S18 DEPT-135 / $^{13}C\{^{1}H\}$ NMR (100.6 MHz) spectrum of Rh[P_2N_2H](COE) (**6**) (in C_6D_6). +/-/x refers to up/down/missing in DEPT-135 spectrum.

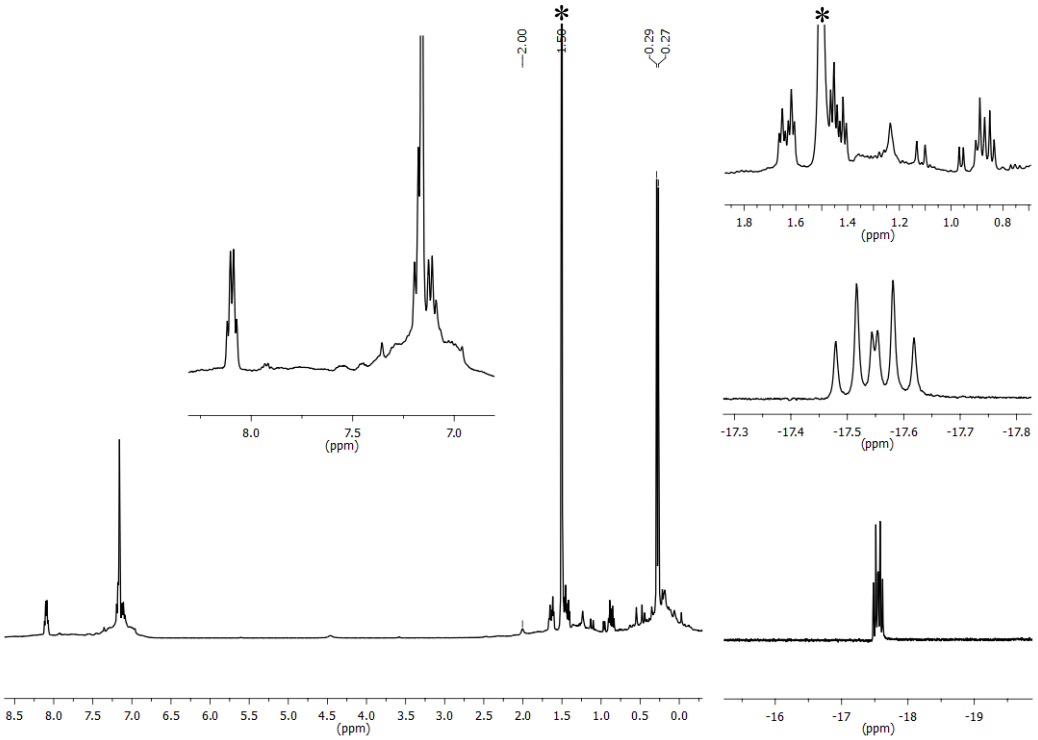

Figure S19 ^{1}H NMR (400 MHz) spectrum of the reaction between Rh[P_2N_2H](COE) (**6**) and H_2 (in C_6D_6). (Resonance denoted with (*) corresponds to cyclooctane formed in the reaction).

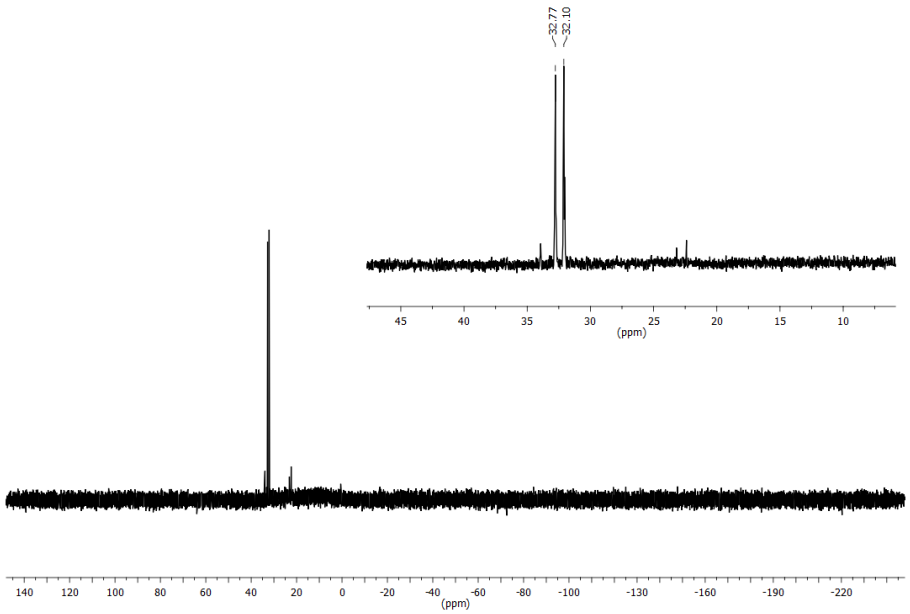

Figure S20 $^{31}P\{^{1}H\}$ NMR (161.9 MHz) spectrum of the reaction between $Rh[P_2N_2H](COE)$ (**6**) and H_2 (in C_6D_6).

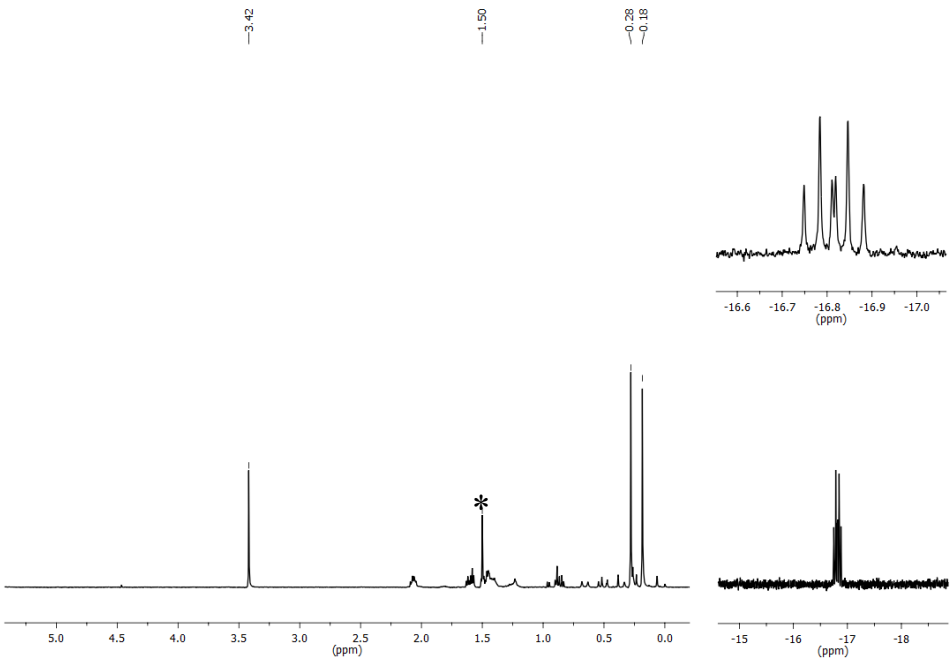

Figure S21 ^{1}H NMR (400 MHz) spectrum of the in-situ sample taken from the reaction of $([Rh(COE)][P_2N_2]Li)_2$(dioxane) (**2**) with H_2 after 4 days (1:1 C_6H_6:C_6D_6; the aromatic region of spectrum was distorted due to the very large C_6H_6 signal and so it is not shown). (Resonance denoted with (*) corresponds to cyclooctane formed in the reaction).

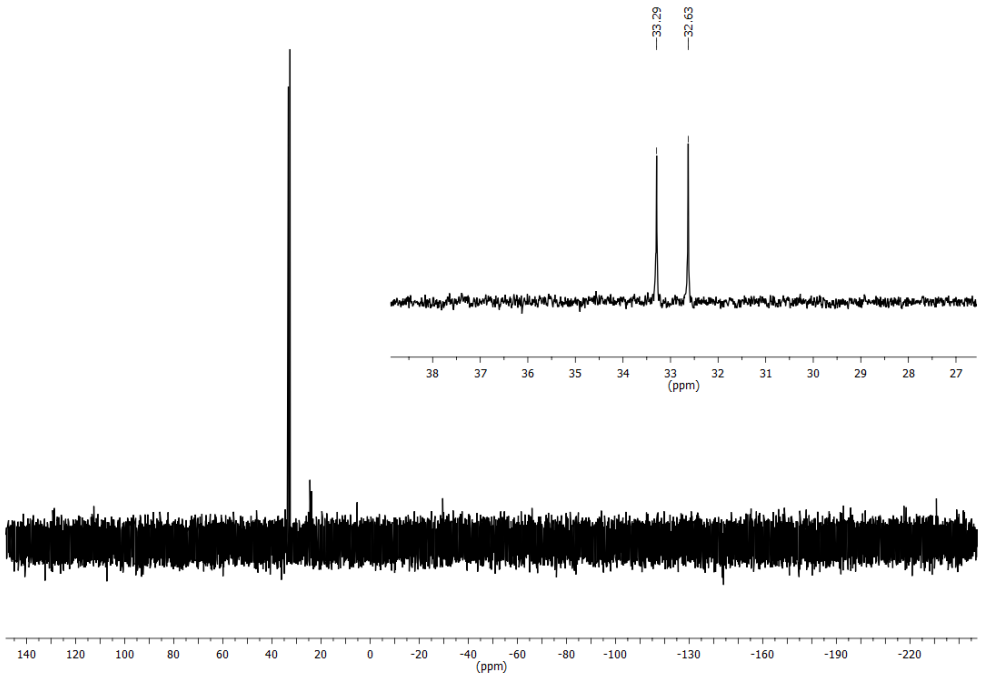

Figure S22 $^{31}P\{^{1}H\}$ NMR (161.9 MHz) spectrum of the in-situ sample taken from the reaction of ([Rh(COE)][P_2N_2]Li)$_2$(dioxane) (**2**) with H_2 after 4 days (1:1 C_6H_6:C_6D_6).

X-ray Crystallographic Analyses

Suitable single crystals were selected, coated in Fomblin oil and mounted on a glass loop. X-ray data was collected on a Bruker DUO or X8 Apex II diffractometer with a graphite-monochromated Mo Kα radiation (λ = 0.71073 Å) at a temperature of 90 or 100 K. Data was integrated using the Bruker SAINT software package.[1] The absorption corrections were performed using the multi-scan technique (SADABS).[2] The structures were solved by direct methods and refined using the Olex2[3] software package with the SHELX refinement program.[4] All non-hydrogen atoms were refined anisotropically. All hydrogen atoms (unless specified) were placed in calculated positions and assigned to an isotropic displacement parameter; the hydrogen atoms bonded to the rhodium atom in $[P_2N_2H]Rh(H)_2$ and $([RhH(Ph)][P_2N_2]Li)_2$-(dioxane) were located in the difference map and were refined isotropically. ORTEPs were generated using ORTEP-3.[5]

CDCC

$[P_2N_2][Rh(COD)]_2$ (**1**)	2005434
$([Rh(COE)][P_2N_2]Li)_2$dioxane (**2**)	2005435
$[P_2N_2H]Rh(H)_2$ (**3**)	2005436
$([Rh(H)_2][P_2N_2]Li)_2$dioxane (**4**)	2004254
$([Rh(C_6H_5)H][P_2N_2]Li)_2$dioxane (**5**)	2004255
$[P_2N_2H]Rh(COE)$ (**6**)	2024716

Table S1 Crystal structure and refinement data for $[P_2N_2][Rh(COD)]_2$ (**2**)

	$[P_2N_2][Rh(COD)]_2$ (**2**)
Chemical formula	$C_{40}H_{66}N_2P_2Rh_2Si_4$
Formula weight	955.06
Crystal system	Monoclinic
Space group	$P2_1/n$
a / Å	10.3474(6)
b / Å	16.4155(12)
c / Å	25.8521(18)
α / °	90
β / °	100.362(2)
γ / °	90
Volume / $Å^3$	4319.6(5)
T / K	90(2)
Z	4
μ / mm^{-1}	0.980
ρ (calcd) / g/cm^3	1.469
F(000)	1984
Absorption correction	Multi–scan
Crystal size / mm	0.17 x 0.09 x 0.08
Wavelength / Å	0.71073
Reflections collected	31583
Unique reflections	7645 (Rint = 0.0572)
Data / restraints / parameters	7645 / 0 / 459
Goodness-of-fit on F^2	0.971
R indices [I >2σ(I)] / R1, wR2	0.0333, 0.0699
R indices (all data) / R1, wR2	0.0559, 0.0779
Completeness to theta max.	0.998
Max. and min. transmission	0.9246, 0.8418
Theta range for data collection / °	2.952 – 50.11

$R1 = \Sigma \; \| F_o | - | F_c \| / \Sigma | F_o |$; $wR2 = [\Sigma \{ w(F_o^2 - F_c^2)^2 \} / \Sigma w(F_o^2)^2]^{1/2}$

Table S2 Crystal structure and refinement data for $([Rh(COE)][P_2N_2]Li)_2$(dioxane) (**2**) and $Rh[P_2N_2H](H)_2$ (**3**)

	$([Rh(COE)][P_2N_2]Li)_2$(dioxane)	$Rh[P_2N_2H](H)_2$
Chemical formula	$C_{68}H_{116}Li_2N_4O_2P_4Si_8Rh_2$	$C_{24}H_{45}N_2P_2Si_4Rh_1$
Formula weight	1594.00	638.83
Crystal system	Monoclinic	Monoclinic
Space group	$P2_1/n$	$P2_1/c$
a / Å	10.7614(5)	15.1347(8)
b / Å	22.3119(13)	10.0758(5)
c / Å	17.1063(8)	20.3672(10)
α / °	90	90
β / °	92.872(2)	95.293(2)
γ / °	90	90
Volume / $Å^3$	4102.2(4)	3092.6(3)
T / K	100(2)	100(2)
Z	2	4
μ / mm^{-1}	0.639	0.827
ρ (calcd) / g/cm^3	1.287	1.372
F(000)	1672	1336
Absorption correction	Multi–scan	Multi–scan
Crystal size / mm	0.27 x 0.17 x 0.17	0.48 x 0.35 x 0.28
Wavelength / Å	0.71073	0.71073
Reflections collected	16275	35414
Unique reflections	7270 (Rint = 0.0405)	9055 (Rint = 0.0269)
Data / restraints / parameters	7270 / 30 / 496	9055 / 0 / 318
Goodness-of-fit on F^2	1.052	1.134
R indices [I >2σ(I)] / R1, wR2	0.0498, 0.1230	0.0231, 0.0649
R indices (all data) / R1, wR2	0.0761, 0.1368	0.0268, 0.0667
Completeness to theta max.	0.972	0.999
Max. and min. transmission	0.8971, 0.6689	0.7933, 0.7095
Theta range for data collection / °	3.65 – 50.628	2.702 – 60.09

$R1 = \Sigma \; \| F_o | - | F_c \| / \Sigma | F_o |$; $wR2 = [\Sigma \{ w(F_o^2 - F_c^2)^2 \} / \Sigma w(F_o^2)^2]^{1/2}$

Table S3 Crystal structure and refinement data for $([Rh(C_6H_5)H][P_2N_2]Li)_2$(dioxane) (**5**) and $([Rh(H)_2][P_2N_2]Li)_2$(dioxane) (**4**)

	$([Rh(C_6H_5)H][P_2N_2]Li)_2$(dioxane)	$([Rh(H)_2][P_2N_2]Li)_2$(dioxane)
Chemical formula	$C_{88}H_{128}Li_2N_4O_2P_4Rh_2Si_8$	$C_{68}H_{120}Li_2N_4O_2Si_8P_4Rh_2$
Formula weight	1842.24	1593.97
Temperature/K	90	90
Crystal system	triclinic	triclinic
Space group	P-1	P-1
a/Å	11.3155(12)	13.1434(14)
b/Å	12.3073(13)	15.766(2)
c/Å	17.4753(18)	19.777(2)
α/°	95.810(7)	101.806(7)
β/°	94.411(7)	108.701(5)
γ/°	103.071(6)	90.185(7)
Volume/Å^3	2345.9(4)	3789.4(8)
Z	1	2
ρ_{calc}g/cm^3	1.304	1.397
μ/mm^{-1}	0.569	0.685
F(000)	968.0	1528
Crystal size/mm^3	0.46 × 0.32 × 0.08	0.48 × 0.16 × 0.04
Radiation	MoKα (λ = 0.71073)	MoKα (λ = 0.71073)
2Θ range for data collection/°	2.354 to 73.384	4.53 to 61.324
Reflections collected	88617	93347
Independent reflections	22948 [R_{int} = 0.0355, R_{sigma} = 0.0334]	28456 [R_{int} = 0.1029, R_{sigma} = 0.0910]
Data/restraints/parameters	22948/0/508	28456/0/738
Goodness-of-fit on F^2	0.805	1.031
Final R indexes [I>=2σ (I)]	R_1 = 0.0293, wR_2 = 0.0977	R_1 = 0.0642, wR_2 = 0.1528
Final R indexes [all data]	R_1 = 0.0364, wR_2 = 0.1066	R_1 = 0.1023, wR_2 = 0.1728
Largest diff. peak/hole / e Å^{-3}	0.91/-0.52	2.88/-1.95

$R1 = \Sigma \| F_o | - | F_c \| / \Sigma | F_o |$; $wR2 = [\Sigma \{w(F_o^2 - F_c^2)^2\} / \Sigma w(F_o^2)^2]^{1/2}$

Table S4 Crystal structure and refinement data for Rh[P_2N_2H](COE) (**6**)

	Rh[P_2N_2H](COE) (**6**)
Chemical formula	$C_{32}H_{57}N_2P_2RhSi_4$
Formula weight	747.00
Temperature/K	90
Crystal system	orthorhombic
Space group	$P2_12_12_1$
a/Å	12.0577(8)
b/Å	16.8079(12)
c/Å	18.6727(14)
α/°	90
β/°	90
γ/°	90
Volume/Å^3	3784.3(5)
Z	4
ρ_{calc}g/cm^3	1.311
μ/mm^{-1}	0.686
F(000)	1576.0
Crystal size/mm^3	0.17 × 0.15 × 0.12
Radiation	MoKα (λ = 0.71073)
2Θ range for data collection/°	4.02 to 61.032
Reflections collected	11527
Independent reflections	11527 [R_{int} = 0.0686, R_{sigma} = 0.0423]
Data/restraints/parameters	11527/0/379
Goodness-of-fit on F^2	1.067
Final R indexes [I>=2σ (I)]	R_1 = 0.0281, wR_2 = 0.0575
Final R indexes [all data]	R_1 = 0.0329, wR_2 = 0.0590
Largest diff. peak/hole / e Å^{-3}	0.42/-0.48

$R1 = \Sigma \| F_o | - | F_c \| / \Sigma | F_o |$; $wR2 = [\Sigma \{w(F_o^2 - F_c^2)^2\} / \Sigma w(F_o^2)^2]^{1/2}$

References

1. *SAINT*, Version 8.18C; Bruker AXS Inc.: Madison, Wisconson, USA, 2012.
2. *SADABS*, Version 2008/1; Bruker AXS Inc.: Madison, Wisconsin, USA, 2008.
3. Dolomanov, O. V.; Bourhis, L. J.; Gildea, R. J.; Howard, J. A. K.; Puschmann, H. *J. Appl. Crystallogr.* **2009,** *42*, 339-341.
4. Sheldrick, G. M. *Acta Cryst. A* **2008,** *64*, 112-122.
5. Farrugia, L. J. *J. Appl. Crystallogr.* **2012,** *45*, 849-854.